Chinese Chemical Letters 31 (2020) 1797–1800

Contents lists available at ScienceDirect

Chinese Chemical Letters

journal homepage: www.elsevier.com/locate/cclet

Communication

# 3D porous acellular cartilage matrix scaffold with surface mediated sustainable release of TGF-$\beta$3 for cartilage engineering

Yixing Huang[a], Xingfang Yu[a], Linjie He[a], Xin Liao[a], Shuo Wang[b,*], Zhiyong Qian[c,*], Liyan Shen[a,*]

[a] Key Laboratory of Orthopedics of Zhejiang Province, Department of Orthopedics, The Second Affiliated Hospital and Yuying Children's Hospital of Wenzhou Medical University, Wenzhou 325000, China
[b] College of Pharmacy, Zhejiang Pharmaceutical College, Ningbo 315199, China
[c] State Key Laboratory of Biotherapy and Cancer Center, West China Hospital, West China Medical School, Sichuan University, and Collaborative Innovation Center for Biotherapy, Chengdu 610041, China

ARTICLE INFO

*Article history:*
Received 16 December 2019
Received in revised form 10 January 2020
Accepted 17 January 2020
Available online 18 January 2020

*Keywords:*
Acellular cartilage matrix scaffold
TGF-$\beta$3
Polyelectrolyte multilayer film
Sustainable release

ABSTRACT

Acellular tissue matrix scaffolds are much closer to tissue's complex natural structure and biological characteristics, thus assess great advantages in cartilage engineering. We used rabbit costal cartilage to prepare acellular microfilaments and further 3D porous acellular cartilage scaffold *via* crosslinking. Poly (L-lysine)/hyaluronic acid (PLL/HA) multilayer film was then built up onto the surface of the resulting porous scaffold. Furthermore, TGF-$\beta$3 was loaded into the PLL/HA multilayer film coated scaffold to obtain a 3D porous acellular cartilage scaffold with sustained releasing of TGF-$\beta$3 up to 60 days. The success of this project will provide a new way for the treatment of articular cartilage defects. Meanwhile, the anchoring and on-site sustained releasing of growth factors mediated by polyelectrolyte multilayered film can also provide a new method for improving the biocompatibility and the biofunctionality for other implanted biomaterials.



Cartilage lesion repair is among one of the big challenges in surgery, since the mature articular cartilage is in lack of vascular and with very limited regeneration ability after damage [1]. Several methods have already been used to improve the cartilage repair, for instance, abrasion arthroplasty, subchondral drilling, microfracture, transplantation of osteochondral plugs, and autologous chondrocyte implantation were among the most used strategies, but very limited success was achieved [2]. Along with the newly development of tissue engineering technique, tissue-engineered articular cartilage has aroused numerous interests and is becoming an important alternative to conventional strategies for cartilage regeneration.

The scaffold is one of the major components in tissue engineering approaches. Many scaffolds, either natural or synthetic, have been used in tissue engineering *in vitro*, as well as *in vivo*, for cartilage repair. Natural scaffolds [3] are functionally superior to non-informational synthetic polymers (*e.g.*, PLGA, PLA, PCL) [4], because they provide both the extracellular matrix (ECM) environment and informational signals (such as the Arg-Gly-Asp also called RGD sequence), these two parameters improve cell attachment and facilitate cell proliferation and even guide cell differentiation. Since the allogenic or xenogeneic cellular antigens were completely removed and most of the structural and functional proteins that constitute the ECM were well preserved, biologic decellularized scaffolds derived from tissue and organs have been successfully used in tissue engineering [5]. A 3D porous scaffold that composed of cartilage ECM should be effective in improving cartilage repair when implanted in the defects [6].

Cell growth factor has many advantages, including low dosage, high specificity and good efficacy, but always easily denaturized in aqueous environment [7]. Transforming growth factor-beta (TGF-$\beta$) plays a major induction role in the numerous growth factors involved in regulating cartilage repair [8]. As for the effective induction of chondrogenesis, the continuous delivery of bioactive TGF-$\beta$ on the defect site over the whole cartilage regeneration period is critically important [9]. To expand its possible clinical applications, suitable biomaterial carriers with high affinity for TGF-$\beta$ to achieve a long-last delivery and to sustain its bioactivity are crucially needed.

Layer-by-layer assembly technology [10] is a method to construct ultra-thin films at the solid-liquid interface by using

* Corresponding authors.
*E-mail addresses:* 16140817@qq.com (S. Wang), anderson-qian@163.com (Z. Qian), shenliyan@wmu.edu.cn (L. Shen).

https://doi.org/10.1016/j.cclet.2020.01.039
1001-8417/

weak interaction forces such as electrostatic and hydrogen bonds. It constructed in mild conditions, and had good repeatability and uniformity; moreover, the film can incorporate a variety of building blocks and can be formed on the surface of scaffolds with irregular and/or porous structures [11]. Meanwhile, the extracellular matrix based poly(L-lysine)/hyaluronic acid (PLL/HA) multilayer membrane has been proved to not only regulate the adhesion behavior of cells on the membrane [12], but also serve as the nano-reservior of growth factors such as bone morphogenetic protein-2 (BMP-2) [13]. Thus, the multilayer film can be an effective coating for immobilizing the growth factors onto the irregular scaffold for long-term sustained releasing.

In this study, the porous scaffold structure was combined with the nano-reservior effect of the layer-by-layer multilayer membrane on growth factors to construct 3D porous decellularized cartilage scaffolds with sustainable TGF-$\beta$3 releasing (Fig. S1 in Supporting information). The decellularized cartilage microfilaments were firstly prepared using the detergent-enzymatic chemical digestion method. Then, the porous cartilage scaffold was constructed *via* freeze-drying and cross-linking. After coating with PLL/HA multilayer, TGF-$\beta$3 was loaded onto the acellular cartilage scaffolds by simply post diffusion. Finally, the sustained releasing behavior of TGF-$\beta$3 *in vitro* was extensively studied. The surface mediated *in situ* release of growth factors by means of layer-by-layer assembly may provide a new strategy for improving the biocompatibility and biofunctionality of implanted biomaterials.

The diameter of cartilage acellular microfilaments was approximately 0.5–10 μm when observed under a microscope, the microfilaments before decellularization contained lots of small black clusters (Figs. 1A and A'), which can be chondrocytes and other extracellular matrix. The clusters disappeared after decellularization, left only microfilaments (Figs. 1B and B'), indicating the cellular compositions were completely removed. After decellularization, its DNA content was $5.92 \pm 0.92$ μg/mg, which is close to the measurement of water control, while the value was $56.64 \pm 6.42$ μg/mg in the normal chondrocytes matrix. The difference in DNA content between the decellularized and undecellularized cartilage groups was statistically significant ($P < 0.05$) (Fig. 1C).

The cartilage acellular matrix scaffolds are generally white and porous mesh, with a diameter of 5 mm and a thickness of 2 mm. The cartilage decellularized scaffolds were observed under stereoscopic microscope and showed a porous network throughout the scaffolds, with uniform distribution of matrix and interconnecting pores (Fig. 2A). To further visualize the surface morphology and confirm the porous structure of the scaffolds, SEM was applied. As shown in Figs. 2B and C, the scaffold was porous with numerous 50–200 μm interconnected pores, and the pores were separated by flat thin plates. To determine the porosity of the scaffolds, the ethanol intrusion method using pycnometer was employed. By carefully weighting the mass of pysnometer and containing ethanol with and without scaffold in constant environment, the porosity of the scaffold was calculated to be as high as $89.5\% \pm 3.41\%$. The highly porosity can greatly facilitate the cell in growth and enhance the drug loading capacity of the scaffolds.

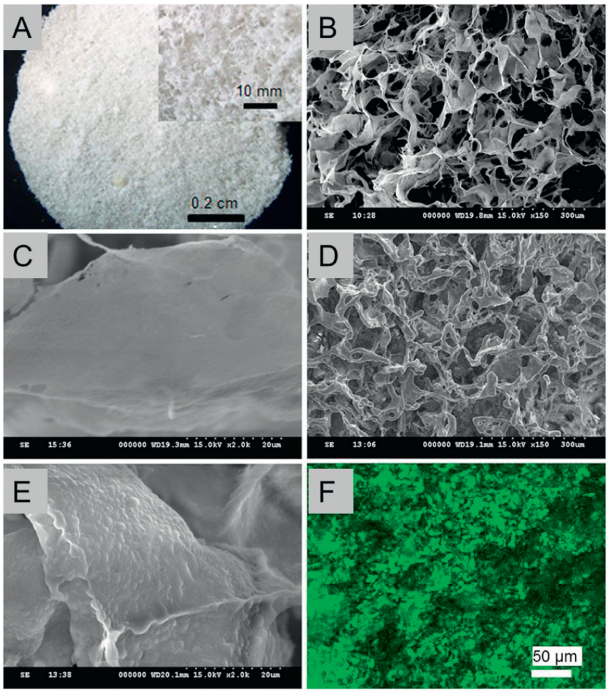


**Fig. 2.** 3D scaffold morphology observed by microscope (A), SEM (B–E) and fluorescence images from CLSM (F). Images for bare scaffold (A–C) and PEM-coated scaffold (D–F). The last layer of PLL was replaced by $PLL^{FITC}$ for CLSM observation (F).

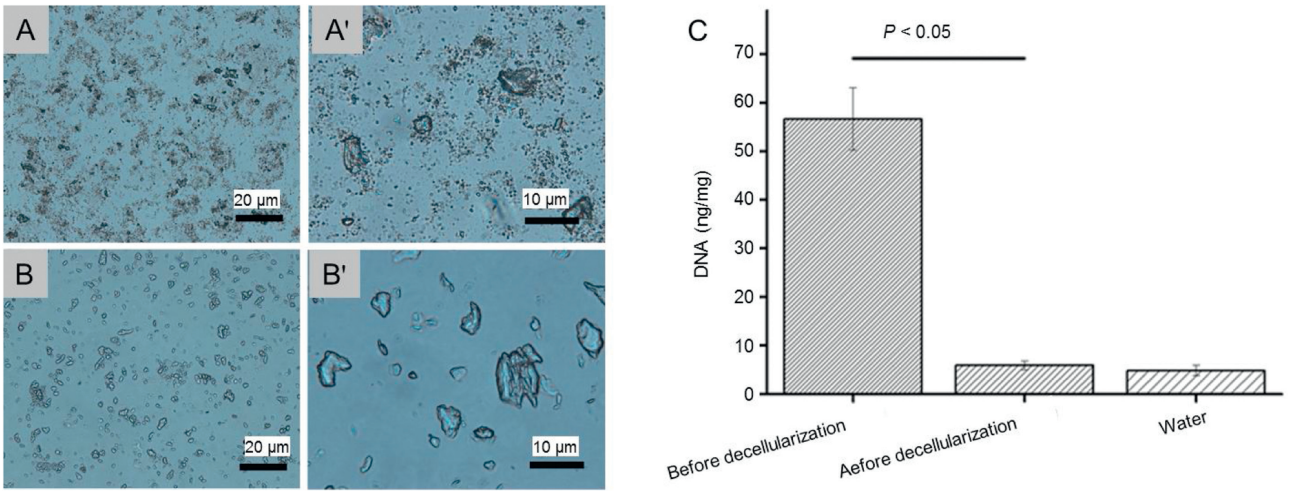


**Fig. 1.** Microscope observations of microfilaments before (A, A') and after (B, B') decellularization. (C) Quantification of DNA content for microfilaments before and after decellularization. Scale bars: 20/10 μm for (A, B)/ (A', B'), respectively.

QCM-D was employed to monitor the LbL assembly of HA/PLL multilayers onto flat substrates, and the frequency shifts ($\Delta F$) and dissipation differences ($\Delta D$) produced at the harmonic of $n = 3$ were plotted against layers deposited (Fig. S2A in Supporting information). Overall, the frequency shifts decreased and dissipation increased steadily as the deposition step increased. Notably, there was a decrease in dissipation and a slightly increase in frequency shift upon the assembly of a PLL layer when the deposited layer pair number excesses 6, suggesting that film densification and water extrusion may occur when PLL molecules were deposited onto HA-terminated films. Film thickness was calculated using Q-tools, as illustrated in Fig. S2B (Supporting information), and film thickness increased exponentially as the layer pair number increased.

The HA/PLL films on the surface of decellularized cartilage scaffolds were examined by scanning electron microscope (SEM) and confocal laser scanning microscope (CLSM) at the microscopic scale. Scanning electron microscopy (SEM) images showed that the multilayered film cover the pores and outer parts of the whole scaffold (Figs. 2D and E) and that the PEM (polyelectrolyte multilayer)-coated decellularized cartilage scaffolds still remained the porous structure (Fig. 2D) but with much thicker separating walls, meanwhile the surface of the HA/PLL multilayer coated decellularized cartilage scaffolds was coarser than that of the unassembled multilayer scaffolds (Fig. 2E). To visualize the multilayer coating on the scaffold under CLSM, the last PLL layer of HA/PLL multilayer was replaced with FITC labeled PLL ($PLL^{FITC}$), uniform fluorescence was observed throughout the whole scaffold in the laser confocal microscope images (Fig. 2F), due to the diffusivity of PLL molecules in PLL/HA film, the last layer of $PLL^{FITC}$ can render the whole film with bright fluorescence. SEM and CLSM images all together proved that the multilayer films coated uniformly on the decellularized cartilage scaffolds both in the pore and on the outer surfaces.

Histological and immunohistological staining was performed on scaffold slides of 10 μm thick to investigate the biological functional matrix remained in the scaffolds, and the data were shown in Fig. 3. All the staining results except DAPI showed that the cartilage decellularized scaffold presented a porous network structure, and the pores in the extracellular scaffold were evenly distributed and interlinked. No blue color was found in either H&E staining (Fig. 3A) or SO staining (Fig. 3B), revealed that chondrocytes were disappeared without the presence of cellular debris and blue-stained nuclear materials. The red color in SO staining results indicated that the preparation of the decellularized scaffold did not cause serious damage to the collagen (Fig. 3B). Blue fluorescence was almost negligible in DAPI staining of chondroacellular matrix scaffolds, and no obvious positive cell components were observed, suggesting complete chondroacellular effect (Fig. 3C). Immunofluorescence examination with collagen II antibodies reconfirmed that collagen II components (Fig. 3D) were well reserved after decellular treatments.

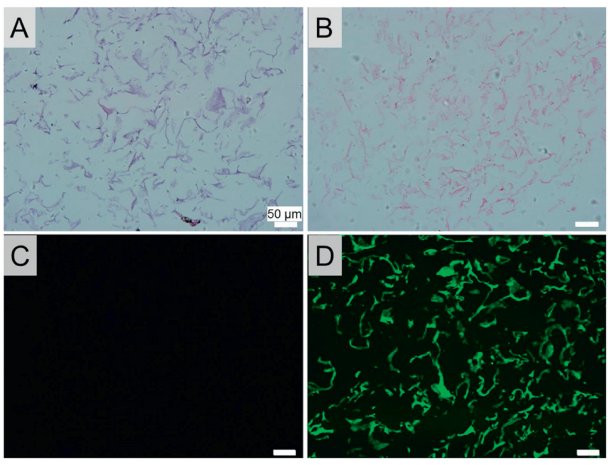


**Fig. 3.** Histology staining for scaffold slide (A) H&E staining, (B) SO staining, (C) DAPI staining and immunofluorescence for Col II (D). The scale bars correspond to 50 μm.

In order to determine TGF-$\beta$3 loading capacity of bare scaffolds and HA/PLL multilayer (both @EDC10 and @EDC50) coated scaffolds, all the scaffolds were loaded TGF-$\beta$3 *via* post-diffusion. The content of TGF-$\beta$3 in the solution before and after scaffold loading was detected by the ELISA kit for every single scaffold. Overall, the initial amounts of TGF-$\beta$3 incorporated in scaffolds before washing ranged between 7−12 μg/scaffold for both film@EDC10 and bare scaffolds while a slightly lower amount was determined for film@EDC50 scaffolds (4−6 μg/scaffold) (Fig. 4A). Furthermore, the TGF-$\beta$3 retention capacity was determined from the kinetics of TGF-$\beta$3 release over 60 days. Unbound and/or loosely bound TGF-$\beta$3 was mostly desorbed after the first wash (for one day), after which much slower release profiles were observed (Figs. 4B and C). This unbound/weakly bound TGF-$\beta$3 represents about 40% of the initial amount loaded for both scaffolds coated with film@EDC50 and film@EDC10, but around 70% for bare scaffold. At the end of the release study (for 60 days), the amounts of TGF-$\beta$3 retained onto the scaffolds were $2.290 \pm 0.025$, $1.642 \pm 0.030$ and $0.398 \pm 0.012$ μg/scaffold for film@EDC10 coated scaffolds, film@EDC50 coated scaffolds and bare scaffolds, respectively (Fig. 4B). These data correspond to 22.45%, 28.56% and 4.88% of the total loaded TGF-$\beta$3 were still kept in the scaffold after 60 days *in vitro* release in PBS (Table 1).

Scaffolds play a central role in regenerative medicine applications by providing optimal three-dimensional environments for cell adhesion, proliferation, and matrix generation [14]. The ideal scaffold should be a functional and structural mimic of the natural extracellular matrix that supports multiple tissue morphogenesis. DNA quantification measurement and DAPI staining results showed no cell fragment and DNA residue in our decellularized scaffolds. Histological analysis of cartilage ECM-derived scaffolds showed that most collagen II was still effectively preserved. The 3D decellularized scaffold had a high porosity up to 90% and all the pores were interconnected. Interconnectivity between pores is advantageous because it facilitates cell migration into the pores and helps the flow of nutrients and metabolic wastes. We further applied the LbL multilayer coating on the three-dimensional decellularized cartilage scaffolds with the attempt to further add to the scaffolds with a reservoir for TGF-$\beta$3. SEM and laser confocal microscope images confirmed that PEM membrane was evenly covered on the decellularized cartilage scaffold and filled the whole pore inside and outside of the scaffolds. The loading and release studies of the scaffolds for TGF-$\beta$3 have shown that the PEM membrane coated three-dimensional acellular scaffold can retain more TGF-$\beta$3 than the bare ones. The sustainable and tunable local release of TGF-$\beta$3 from biocompatible 3D decellularized cartilage scaffolds was realized thereby. The chondrogenic induction property of the scaffold was verified in the cartilage defect model in rats (Figs. S3-6 in Supporting information), the results showed that the release TGF-$\beta$3 is bioactive and the scaffolds that sustainably release TGF-$\beta$3 significantly augmented the cartilage repair.

In conclusion, 3D porous acellular cartilage scaffold was made from rabbit costal cartilage by decellular treatment and followed by chemical crosslinking. The decellularized scaffolds retained most of the cartilage ECM components and had interconnected porous structures with porosity up to 90%. Poly(L-lysine)/hyaluronic acid (PLL/HA) multilayered films were successfully deposited on the scaffolds both on surfaces and in the pores *via* facial LbL

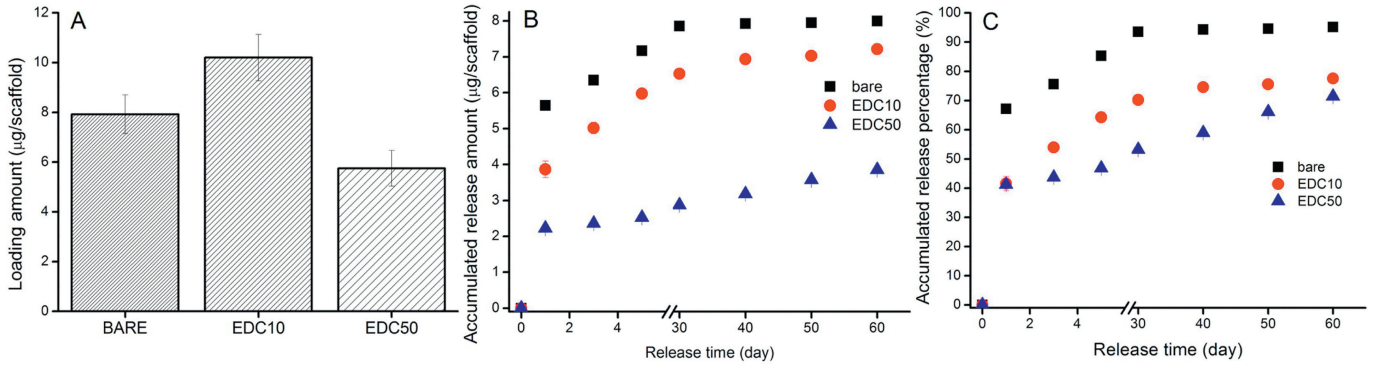


**Fig. 4.** TGF-$\beta$3 loading (A) amount and release profiles (B, C) for bare scaffolds (■), scaffolds coated with @EDC10 film (●), and scaffolds coated with @EDC50 film (▲).

**Table 1**
TGF-$\beta$3 loading and release amount for different scaffolds.

| TGF-$\beta$3 loading and release | Initial loading amount (μg/scaffold) | First rinse release amount (μg/scaffold) | First rinse release (%) | Final remaining amount (μg/scaffold) | Final remaining (%) |
|---|---|---|---|---|---|
| Bare scaffold | 7.925 ± 0.776 | 5.642 ± 0.054 | 67.17 | 0.398 ± 0.012 | 4.88 |
| @EDC10 | 10.20 ± 0.935 | 3.867 ± 0.228 | 41.59 | 2.290 ± 0.025 | 22.45 |
| @EDC50 | 5.75 ± 0.716 | 2.227 ± 0.055 | 41.25 | 1.642 ± 0.030 | 28.56 |

The TGF-$\beta$3 loading concentration is 50 μg/mL.

manner. The PEM-coated scaffolds then sequestered significant amounts of TGF-$\beta$3, which underwent sustainable local release up to 60 days when immersed in PBS. To our knowledge this is the first time in the research to achieve such a long-term release for a chondrogenic protein, and more importantly the released protein was biologically active. Furthermore, the TGF-$\beta$3 loading amount and subsequent delivery behavior can be adjusted by tuning the crosslink level of PEM coating on the scaffolds, providing the possibility for precise and personalized medicine. The 3D porous decellularized cartilage scaffold with PEM coating and surface mediated sustainable TGF-$\beta$3 releasing is a suitable candidate for chondrocyte repopulation and thus provide an alternative for cartilage engineering.

## Declaration of competing interest

The authors declare that they have no known competing financial interests or personal relationships that could have appeared to influence the work reported in this paper.

## Acknowledgments

The financial support from the National Natural Science Foundation of China (No. 41506091), Zhejiang Provincial Public Welfare Project (No. 2017C33035), Wenzhou Science & Technology Bureau (Nos. Y20170091, Y20190021), Health Commission of Zhejiang Province (No. 2019KY465), and Key Laboratory of Orthopaedics of Zhejiang Province (No. ZJGK1806Y) are well acknowledged.

## Appendix A. Supplementary data

Supplementary material related to this article can be found, in the online version, at doi:https://doi.org/10.1016/j.cclet.2020.01.039.

## References

[1] (a) E. Hunziker, Osteoarthr. Cartilage 7 (1999) 15–28;
(b) D.A. Sacolick, J.C. Kirven, M.M. Abouljoud, J.S. Wverhart, D.C. Flanigan, J. Knee Surg. 32 (2019) 1102–1110.
[2] T.M. Simon, D.W. Jackson, Sports Med. Arthrosc. 14 (2006) 146–154.
[3] (a) F. Bolland, S. Korossis, S.P. Wilshaw, et al., Biomaterials 28 (2007) 1061–1070;
(b) L. Flynn, G.D. Prestwich, J.L. Semple, K.A. Woodhouse, Biomaterials 28 (2007) 3834–3842.
[4] T. Wu, M. Ding, C. Shi, et al., Chin. Chem. Lett. 31 (2020) 617–625.
[5] Q. Yao, Y.W. Zheng, Q.H. Lan, et al., Mat. Sci. C-Mater. 104 (2019) 109942.
[6] (a) S.F. Badylak, Transpl. Immunol. 12 (2004) 367–377;
(b) Y. Li, Y. Liu, X. Xun, et al., ACS Appl. Mater. Interface 11 (2019) 36359–36370.
[7] C. Guo, X. Guo, W. Chu, N. Jiang, H. Li, Chin. Chem. Lett. 30 (2019) 1302–1306.
[8] F. Barry, R.E. Boynton, B. Liu, et al., Exp. Cell Res. 268 (2001) 189–200.
[9] (a) A.K. Asen, L. Goebel, A. Rey-Rice, et al., FASEB J. 32 (2018) 5298–5311;
(b) Y.R. Chen, Z.X. Zhou, J.Y. Zhang, et al., Front. Chem. 7 (2019) 745.
[10] G. Decher, Science 77 (1997) 1232–1237.
[11] (a) C. Picart, Ph. Lavalle, P. Hubert, et al., Langmuir 17 (2001) 7414–7424;
(b) Q. Tang, Z. Hu, H. Jin, et al., Theranostics 9 (2019) 1125–1143;
(c) D. Yan, L.L. Qiu, Y.F. Wang, et al., Chin. Chem. Lett. 29 (2018) 922–926.
[12] (a) M.P. Sousa, E. Arab-Tehrany, F. Cleymand, J.F. Mano, Small 15 (2019) 1901228;
(b) K.F. Ren, M. Hu, H. Zhang, et al., Prog. Polym. Sci. 92 (2019) 1–34;
(c) P. Machillot, C. Quintal, F. Dalonneau, et al., Adv. Mater. 30 (2019) 1801097.
[13] (a) F. Gilde, L. Fourel, R. Guillot, et al., Acta Biomater. 46 (2016) 55–67;
(b) M. Bouyer, R. Guillot, J. Lavaud, et al., Biomaterials 104 (2016) 168–181.
[14] (a) A. Ho-Shui-Ling, J. Bolander, L.E. Rustom, et al., Biomaterials 180 (2018) 143–162;
(b) Q. Wang, J. Xu, H. Jin, et al., Chin. Chem. Lett. 28 (2017) 1801–1807.